THE JOURNAL OF PHYSICAL CHEMISTRY B

Article

pubs.acs.org/JPCB

The Prospect of Selective Recognition of Nerve Agents with Modular Basket-like Hosts. A Structure–Activity Study of the Entrapment of a Series of Organophosphonates in Aqueous Media

Yian Ruan, Hashem A. Taha, Ryan J. Yoder, Veselin Maslak, Christopher M. Hadad,* and Jovica D. Badjić*

Department of Chemistry and Biochemistry, The Ohio State University, 100 West 18th Avenue, Columbus, Ohio, United States

Supporting Information

ABSTRACT: We designed, prepared, and characterized three cup-shaped cavitands **1**–**3** for trapping organophosphonates (O═PR(OR′)$_2$, 118–197 Å^3) whose shape and size correspond to G-type chemical warfare agents (132–186 Å^3). With the assistance of computational (molecular dynamics) and experimental (^{1}H NMR spectroscopy) methods, we found that host [**1**–**H**$_3$]$^{3+}$ orients its protonated histamine residues at the rim outside the cavity, in bulk water. In this unfolded form, the cavitand traps a series of organophosphonates **5**–**13** (K_{app} = 87 ± 1 to 321 ± 6 M^{-1} at 298.0 K), thereby placing the P–CH$_3$ functional group in the inner space of the host. A comparison of experimental and computed ^{1}H NMR chemical shifts of both hosts and guests allowed us to derive structure–activity relationships and deduce that, upon the complexation, the more sizable P–OR functional groups in guests drive organophosphonates to the northern portion of the basket [**1**–**H**$_3$]$^{3+}$. This, in turn, causes a displacement of the guest's P–CH$_3$ group and a contraction of the cup-shaped scaffold. The proposed induced-fit model of the recognition is important for turning these modular hosts into useful receptors capable of a selective detection/degradation of organophosphorus nerve agents.

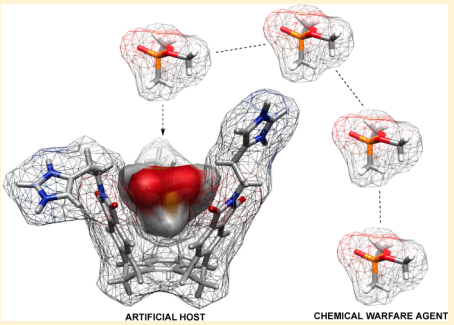

INTRODUCTION

Sarin (GB), soman (GD), tabun (GA), and VX agents are organophosphorus (OP, Figure 1) compounds, developed in the last century as chemical warfare agents (CWAs).[1,2] These substances[3] are highly toxic to humans[4,5] due to their ability to inhibit the action of the enzyme acetylcholinesterase (AChE) in the postsynaptic membrane at neuromuscular junctions.[6−8] Markedly, the loss of AChE function causes an accumulation of the acetylcholine neurotransmitter, which upon a prolonged exposure to nerve agents leads to respiratory malfunction (asphyxiation) and death; for instance, it has been estimated that inhalation of 50–100 ppb of sarin gas for 1 min is lethal![9]

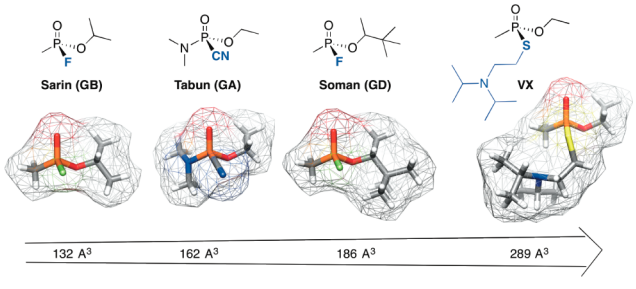

Figure 1. Chemical structure of G- and V-type nerve agents (top), along with their van der Waals surface (Chimera). Note that the sizes and shapes are changing in the series (MMFFs, Spartan).

Since G- and V-type agents (Figure 1) are stored in vast quantities around the world,[10] there is a potential for their use in terrorist attacks against both military and civilian personnel. A method for the rapid detection of small amounts[11] of OPs in the gas (as vapor), liquid (as in water), or solid (as in ground) phase is therefore essential[12] for preventing the occurrence of tragic events. The development of effective degradation and decontamination procedures[13−15] has been a priority for years, yet there is also a need for catalytic methods for the hydrolysis/oxidation[16−18] of OP nerve agents. Currently, the unambiguous detection of CWAs requires expensive instrumentation such as gas chromatography, mass spectrometry, and/or NMR spectroscopy, and portability is an additional challenge.[19−22] Correspondingly, analytical methods based on color changes are particularly attractive toward developing a versatile chemosensor of CWAs.[23−31] In essence, the substitution of a good leaving group (X = F, CN, SR; Figure 1) on the electrophilic phosphorus with a strong nucleophile[32] is typically utilized to give a distinctive optical signal and thereby indicates the presence of toxic materials.[33−35] Most colorimetric chemosensors are, however, prone to "false alarms" due to the absence of selectivity by which the "chemical activation" takes place: any good electrophile present in the area may

Received: February 21, 2013
Revised: February 26, 2013
Published: February 27, 2013

trigger the desired response of current chromogenic chemosensors. Indeed, discriminating nerve gases with an array of colorimetric molecules[36] (optoelectronic nose)[37,38] could, in principle, address the problem of chemoselectivity, yet this powerful methodology will certainly benefit from incorporating molecular recognition[39] as an element of design in the system.[40] In accord with this reasoning, trapping CWAs with a concave host[41] is likely to provide a desired chemoselective discrimination for creating suitable sensing devices. Still, there is insufficient fundamental understanding of the recognition of CWAs with cavitands[42,43] to impede further developments in the field. Early studies with cyclodextrins[44] have shown that these concave hosts have an ability to promote a degradation of sarin (α-cyclodextrin)[45,46] and soman (β-cyclodextrin)[47,48] via encapsulation. Moreover, β-cyclodextrin derivatives with nucleophilic groups at the wide and narrow rims of the host were found to react with paraoxon, cyclosarin (GF), and tabun (GA) at an accelerated rate (faster than background reactions).[49−51] Importantly, Dalcanale and co-workers have recently reported[52] a solid-state structure of a calix[4]arene cavitand hosting dimethyl methylphosphonate (DMMP, Figure 2) as a guest and with one OCH_3 group forming an attractive C−H···π interaction with the host's cavity. Furthermore, these calixarene hosts were immobilized on various surfaces for permitting selective detection of DMMP vapors with exceptional sensitivity.[53] Thus, complexation of a nerve agent by a functional cavitand may allow for unambiguous detection of these toxic substances, along with the prospect of promoting their effective degradation. An objective of our study is to elucidate details of the complexation of a series of organophosphonate compounds with modular basket-like[54−56] hosts (Figure 2A). Will a cup-shaped cavitand of type $[\mathbf{1}-\mathbf{H}_3]^{3+}$ (Figure 2A) bind to OP compounds in water, and if so, what is the nature of that interaction? Using methods of computational and experimental chemistry, we hereby establish that our molecular baskets (Figure 2A) are complementary to OP compounds and have a disposition for entrapping these chemicals. The mode of the interaction is unique, with both theory and experiment suggesting: (a) the importance of P−CH_3 functionality for the binding and (b) an induced-fit mechanism of the inclusion complexation.

EXPERIMENTAL SECTION

General Information. All chemicals were purchased from commercial sources and used as received, unless stated otherwise. All solvents were dried prior to use according to standard literature procedures. Chromatography purifications were performed using silica gel 60 (SiO_2, Sorbent Technologies 40−75 μm, 200 × 400 mesh). Thin-layer chromatography (TLC) was performed on silica-gel plate w/UV254 (200 μm). Chromatograms were visualized by UV-light and stained using 20% phosphomolybdic acid in ethanol, if needed. All NMR samples were prepared in J. Young Valve NMR Tubes purchased from Norell. ^{1}H and ^{13}C NMR spectra were recorded, at 400 and 100 MHz, respectively, on a Bruker DPX-400 spectrometer, unless otherwise noted. They were referenced using the solvent's residual signal as an internal standard. NMR samples were prepared using $CDCl_3$, CD_2Cl_2, and CD_3OD and used as purchased from Cambridge Isotope Laboratories. The chemical shift values are expressed as δ values (ppm), and the couple constant values (J) are in Hertz (Hz). The following abbreviations were used for signal multiplicities: s, singlet; d, doublet; t, triplet; m, multiplet; and br, broad. For NMR measurements, the temperature was corrected with neat methanol as a standard. HRMS (ESI) were measured on a Micromass Q-Tof II spectrometer. Microcalorimetric experiments were performed with an isothermal titration calorimeter (Nano-ITC). The heat of the reaction was corrected for the dilution of the guest's solution. Computer simulations (curve fitting) were performed with simulation software provided by TA Instruments.

Synthetic Procedures. To a suspension of *tris*-anhydride (5.0 mg, 7.9 mmol) dissolved in 0.5 mL of dimethyl sulfoxide (DMSO), histamine (2.3 mg, 23.7 mmol) was added. After an addition of 50 μL of anhydrous pyridine, the solution was kept at 125 °C for 12 h. The mixture was concentrated under reduced pressure, and the residue was purified with thin-layer chromatography (SiO_2, CH_3OH) to yield basket **1** as a white solid (3.0 mg, 42%). ^{1}H NMR (400 MHz, CD_3OD, 300 K): δ = 7.63 (s, 6H), 7.42 (s, 3H), 6.69 (s, 3H), 4,71 (s, 6H), 3,74 (t, J = 7.2 Hz, 6H), 2.81 (t, J = 7.2 Hz, 6H), 2.59 (m, 6H); ^{13}C NMR (100 MHz, CD_3OD, 300 K): δ = 169.8, 158.9, 139.5, 136.1, 131.7, 117.0, 66.9, 50.3, 38.9, 26.7 ppm; HRMS ESI: m/z calcd for $C_{54}H_{39}N_9O_6$: 910.3102 $[M+H]^+$, found: 910.3122.

Tris-anhydride (3.0 mg, 4.8 mmol) and β-alanine (1.3 mg, 14.4 mmol) were added to 0.5 mL of DMSO. The mixture was kept at 125 °C for 2 h and then concentrated under reduced pressure. The solid residue was purified with thin-layer chromatography (SiO_2, CH_3OH:CH_2Cl_2 = 1:1) to yield basket **2** as a white solid (2.1 mg, 52%). ^{1}H NMR (400 MHz, $CDCl_3$/CD_3OD, 300 K): δ = 7.54 (s, 6H), 4.58 (s, 6H), 3,79 (s, 6H), 2.62 (m, 12H); ^{13}C NMR (150 MHz, $CDCl_3$/CD_3OD, 300 K): δ = 168.5, 157.1, 138.1, 130.5, 116.3, 65.3, 33.7, 32.7, 29.8 ppm; HRMS ESI: m/z calcd for $C_{48}H_{33}N_3O_{12}$: 866.1962 $[M + Na]^+$, found: 866.1986.

To a suspension of *tris*-anhydride (5.0 mg, 7.9 mmol) in 0.5 mL of DMSO was added ethanolamine (1.5 μL, 23.7 mmol). After an addition of 50 μL of anhydrous pyridine, the solution was kept at 125 °C for 12 h. The mixture was concentrated under reduced pressure, and the residue was purified with thin-layer chromatography (SiO_2, CH_3OH:CH_2Cl_2 = 1:7) to yield basket **3** as a white solid (3.8 mg, 63%). ^{1}H NMR (400 MHz, $CDCl_3$/CD_3OD, 300 K): δ = 7.63 (s, 6H), 4.69 (s, 6H), 3.63 (m, 12H); ^{13}C NMR (100 MHz, $CDCl_3$/CD_3OD, 300 K): δ = 168.8, 157.0, 138.0, 130.3, 116.1, 65.3, 59.7, 40.0 ppm; HRMS ESI: m/z calcd for $C_{45}H_{33}N_3O_9$: 782.2114 $[M + Na]^+$, found: 782.2108.

Generation of Conformational Ensemble. A Monte Carlo computational protocol was used to generate random structures, which were optimized with the AMBER* force field included in the MacroModel software. From these structures, 10 were chosen for additional geometry optimizations: the five lowest energy structures were examined first, then five additional conformations were chosen to adequately represent the conformational space by examining the orientation of the histimine arms of the basket. For nine of the ten conformations (one conformation could not be optimized), partial atomic charge calculations were performed using the Merz−Kollman scheme (B3LYP/6-31+G*//B3LYP/6-31+G*); charges were averaged over all conformations. Solvated molecular dynamics (MD) simulations were run for 5 ns in explicit TIP3P water on the 9 conformations with averaged charges using the *sander* module in the AMBER program (starting coordinates are included in Supporting Information). A three-step equilibration scheme was performed: an initial minimization step where only the positions of solvent molecules were relaxed was followed by

dx.doi.org/10.1021/jp401841w | J. Phys. Chem. B 2013, 117, 3240−3249

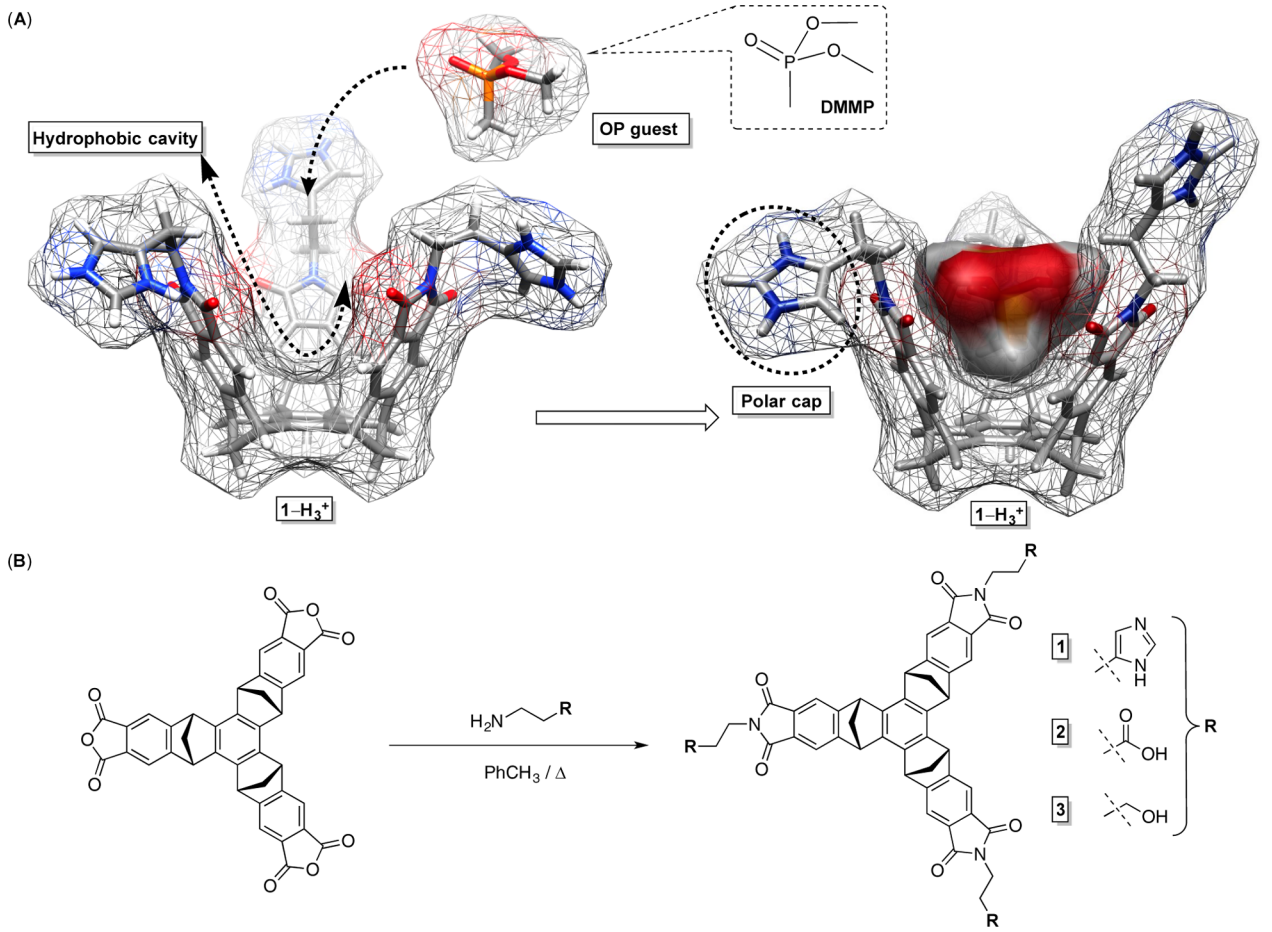

Figure 2. (A) van der Waals surfaces of $[\mathbf{1}{-}\mathbf{H}_3]^{3+}$ and dimethyl methylphosphonate **5** (DMMP, Spartan/MMFFs) demonstrate shape complementarity of this host/guest pair. (B) Baskets **1**–**3** were prepared by condensation of *tris*-anhydride[57] and functionalized amines.

minimization of the system as a whole; the system then underwent a heating phase from 0 to 300 K with a small restraint on the basket to prevent drastic fluctuations in structure. The volume was kept constant, and the SHAKE algorithm was used to constrain bonds involving hydrogen atoms. Production dynamics were run over 5 ns using NPT conditions. Long-range electrostatic interactions were calculated using the particle mesh Ewald (PME) algorithm with a cutoff of 10 Å. The energy trajectories for each of the MD runs are shown in Figure S17.

Molecular Docking Simulations. The resulting MD trajectories were aligned and combined, and a clustering analysis was done using the *ptraj* module of AMBER. Ten clusters were obtained, and these snapshots (coordinates follow) were used for our rigid docking simulations, which were completed using Autodock 4.0, where all rotatable bonds on the guest molecules were allowed to rotate and the basket remained rigid. Molecular dynamics simulations of the lowest energy pose and/or most populated pose of each guest from each of the 10 docking simulations were performed for 8 ns in a box of TIP3P water molecules. We monitored the dynamics of the guest–basket complex as a function of time. Initially, we looked at the dynamics of dimethyl methylphosphonate guest (**5**) within each of the different basket snapshots and found that regardless of the starting orientation, the guest eventually equilibrates to have the P–Me group pointing toward the base of the basket. This can be seen clearly by monitoring the distance between the center of the basket base and the alkyl group carbon (Figure S20). Guests with larger alkyl groups also preferred to have these groups pointed toward the hydrophobic base of the basket, and as the size of the alkyl group increases, the propensity for the guest to be in this orientation also increases.

NMR Calculations. A series of structures were created by varying the dihedral angle α of the basket (2° increments up to 28°, Figure S21/Figure 6A). Each structure was optimized at the mPW1PW91/6-31G* level of theory while retaining C_{3v} symmetry of the host (energy profile is shown in Figure S22). Single point energies and NMR parameters were computed on these optimized structures using the mPW1PW91/6-311+G** level of theory. These calculations were carried out in the gas phase as well as with the polarizable continuum model for chloroform. Isotropic chemical shift values and coupling constants were extracted from the output files, and the changes in chemical shift (Figure S23, A) and coupling constant (Figure S23, B) are plotted as a function of increasing cavity size. There were no differences found between the calculations in the gas phase and chloroform (<0.3 Hz differences).

RESULTS AND DISCUSSION

Working Hypotheses. Molecular baskets of type $[\mathbf{1}{-}\mathbf{H}_3]^{3+}$ are C_3 symmetric hosts[57−59] that are complementary to tetrahedral organophosphonate guests (Figure 2A).[60] In a polar, aqueous environment, the guest is anticipated to place one of its hydrophobic groups inside the nonpolar basket's interior, and with the remaining three units pointing to the side

dx.doi.org/10.1021/jp401841w | J. Phys. Chem. B 2013, 117, 3240−3249

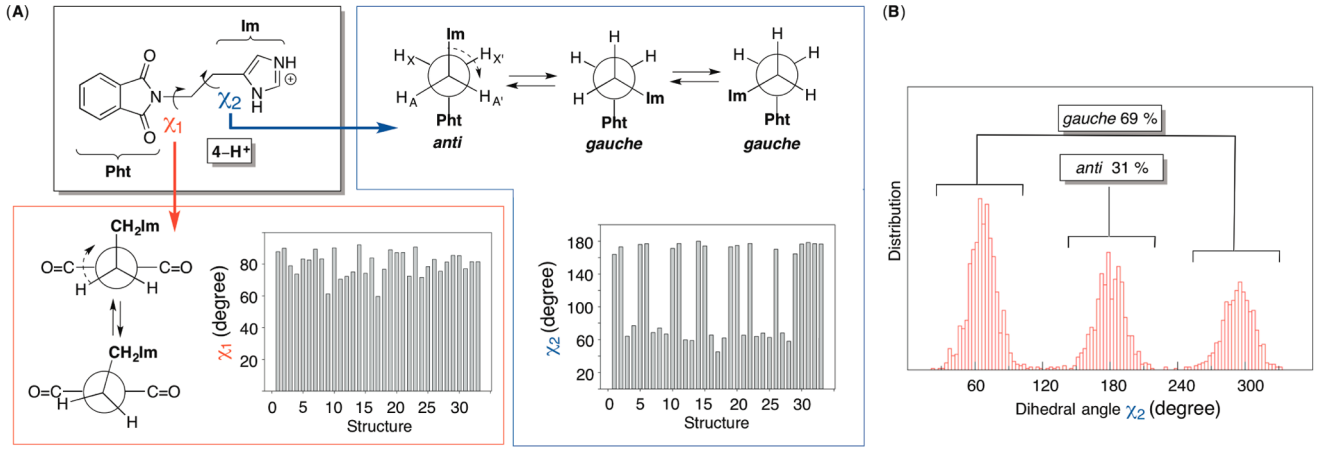

Figure 3. (A) Chemical structure of model compound $[\mathbf{4}{-}\mathbf{H}]^+$ and the Newman projections of its rotamers about χ_1 (red square) and χ_2 (blue square) torsion angles. Examination of 33 structures from the Cambridge Structural Database shows preferred orientations about χ_1 and χ_2 torsions within various Pht$-CH_2-CH_2-$R molecules. (B) Molecular dynamics (AMBER 11) calculations of $[\mathbf{4}{-}\mathbf{H}]^+$ in water suggest an almost statistical distribution of anti/gauche conformers.

apertures of the host (Figure 2A). Desolvation of the organophosphonate guests, in addition to the cup-shaped inner space, should serve as a driving force for the complexation (via the hydrophobic effect).[61−64] Furthermore, only properly sized groups can fit in the hydrophobic pocket so as to impart selective recognition. The functional appendages at the rim (Figure 2A) may assist the complexation by forming supplementary noncovalent interactions with the guest. In our study, however, these groups were envisioned to enable the basket's solubility in water. To test our working hypotheses, we decided to investigate the interaction of baskets **1**−**3** (Figure 2B) with a series of differently sized alkyl dialkylphosphonates (vide infra) in water. Baskets comprise basic (**1**, R = $C_3H_3N_2$), acidic (**2**, R = CO_2H), and neutral (**3**, R = OH) groups at the periphery, resembling amino acids histidine (His), aspartic acid (Asp), and serine (Ser), respectively. Phosphonate guests (**5**−**13**, 118−197 Å^3; Figures 8 and 9) were chosen so that their size and shape correspond to G-type nerve agents (132−186 Å^3, Figure 1).

Synthesis. The condensation of *tris*-anhydride[57] with histamine, 3-aminopropanoic acid, or ethanolamine gave baskets **1**−**3**, respectively, in 42−63% yield (Figure 2B). Model compound **4** (Figure 3) was obtained by condensation of phthalic anhydride and histamine in toluene.[65] Organophosphonate guests **7**,[66] **9**, **11**, and **12**[67,68] were synthesized in accord with literature protocols.

Aqueous Solubility and Conformational Analysis. All three baskets **1**−**3** were found to be soluble in CD_2Cl_2/CH_3OH, but practically insoluble in water. We attempted to dissolve these compounds by adjusting the pH of the water solution (from 1 to 14), but even after a prolonged sonication of the heterogeneous mixture, there was no desired dissolution. Ultimately, we added an excess of trifluoroacetic acid (TFA) to **1** in CH_2Cl_2/CH_3OH. Upon evaporation of the solvent, the presumed compound $[\mathbf{1}{-}\mathbf{H}_3]^{3+}$ $[CF_3CO_2^-]_3$ was subsequently dissolved in 10.0 mM phosphate buffer (pH = 2.5 ± 0.1). The ^{19}F NMR spectrum of the solution showed the presence of ∼4 equivalents of trifluoroacetate (Figure S1). We found that an excess of TFA would remain despite the solid being kept at a high temperature and under vacuum for a prolonged period of time. Markedly, the described method did not give satisfactory results with baskets **2** and **3**; thus, we studied the recognition behavior of $[\mathbf{1}{-}\mathbf{H}_3]^{3+}$.

To understand the conformational characteristics of basket $[\mathbf{1}{-}\mathbf{H}_3]^{3+}$ and its preorganization,[60] we first examined the model compound $[\mathbf{4}{-}\mathbf{H}^+]$ (Figure 3A). This molecule is virtually a double rotor with two torsional degrees of freedom χ_1 and χ_2 (Figure 3A). The examination of solid-state structures of 33 phthalimide derivatives of type Pht$-CH_2-CH_2-$R (Cambridge Structural Database, CSD) revealed a conformational bias about the 6-fold χ_1 torsion: the variation of the χ_1 angle from 60 to 92°, with a disposition toward χ_1 = 80 ± 8° (mean ± standard deviation), indicates a rather small energetic penalty for the formation of eclipsed or staggered geometries (Figure 3A). The conformational isomerism about the CH_2-CH_2 bond is, within the examined 33 structures, unbiased with an almost equal population of gauche (χ_2 = 60°, Figure 3A) and anti (χ_2 = 180°, Figure 3A) states. Interestingly, the X-ray structure of *N*-(2-imidazol-4-ylethyl)phthalimide **4** has an anti conformation (χ_2 ∼ 180°) in the solid state.[65] A molecular dynamics (MD) simulation (10 ns, AMBER) of $[\mathbf{4}{-}\mathbf{H}^+]$ in water suggested a preference for gauche (χ_2 = 60/300°, Figure 3B) conformers at equilibrium (69%, Figure 3B). The ^{1}H NMR spectrum of $[4{-}H^+]$ showed a single set of resonances (CD_2Cl_2, 400 MHz), even at low temperatures (206−301 K, Figure S2). A rapid rotation of the molecule about its three central bonds would average out the ^{1}H NMR resonances of the phthalimide and imidazole rings. Two CH_2 groups in $[\mathbf{4}{-}\mathbf{H}^+]$, however, each gave a triplet characterized with the apparent scalar coupling of J = 6.6 Hz (Figure S2). Importantly, the ^{1}H NMR appearance of AA'XX' spin systems[69] is, in the X$-CH_2-CH_2-$Y fragments, a function of the anti/gauche ratio of the conformers: for a mixture of the two states,[70,71] it has been computed[72] that J_{AX} approaches $J_{AX'}$ (via averaging the coupling constants) so that the signal pattern simplifies into a pair of triplets (A_2X_2, $\Delta\nu_{AX} \gg J_{AX}$). While the appearance of a more complex NMR pattern, corresponding to the X$-CH_2-$ CH_2-Y fragment, would manifest a great dominance of either anti or gauche conformers,[72] we conclude that the experimental result is in line with our theoretical studies.

The two torsional degrees of freedom (χ_1 and χ_2) determining the position of the imidazole ring in model compound $[\mathbf{4}{-}\mathbf{H}^+]$ are also present in basket $[\mathbf{1}{-}\mathbf{H}_3]^{3+}$ (Figure

dx.doi.org/10.1021/jp401841w | J. Phys. Chem. B 2013, 117, 3240−3249

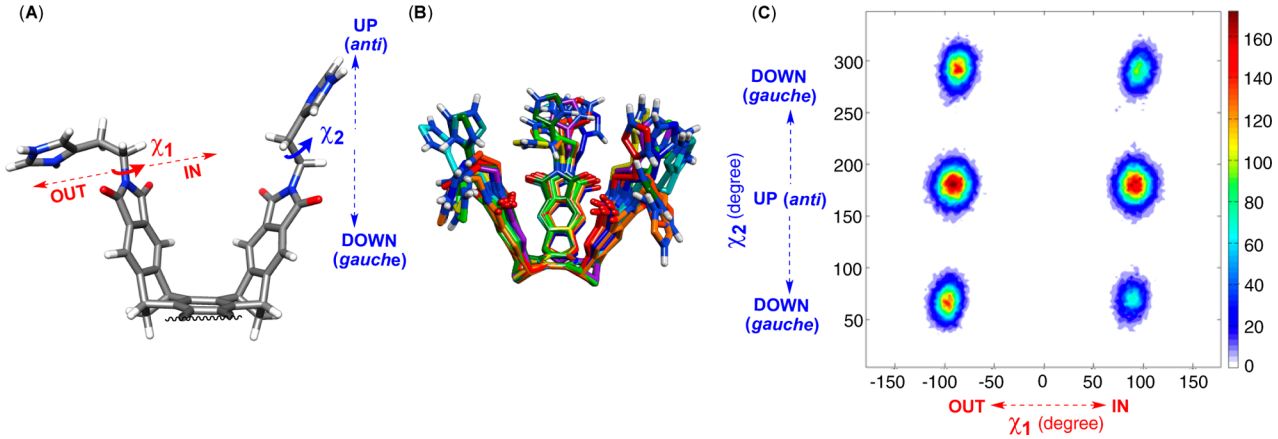

Figure 4. (A) Three imidazole rings in $[\mathbf{1}{-}\mathbf{H}_3]^{3+}$ adopt different positions with respect to the cup-shaped platform: the rotation about the $CH_2{-}CH_2$ bond (χ_2) gives anti (UP) and gauche (DOWN) conformers, while the rotation about the $N{-}CH_2$ bond (χ_1) gives IN and OUT conformers. (B) Ten major conformational states of $[\mathbf{1}{-}\mathbf{H}_3]^{3+}$ were identified by a clustering analysis of molecular dynamics (MD) trajectories based on an RMSD protocol using the ptraj module of AMBER. (C) The contour plot depicts a computed conformational distribution of $[\mathbf{1}{-}\mathbf{H}_3]^{3+}$ in water (MD, AMBER); in the third dimension, the white designates the absence of conformational states, while the red correspond to the highest population of conformational states.

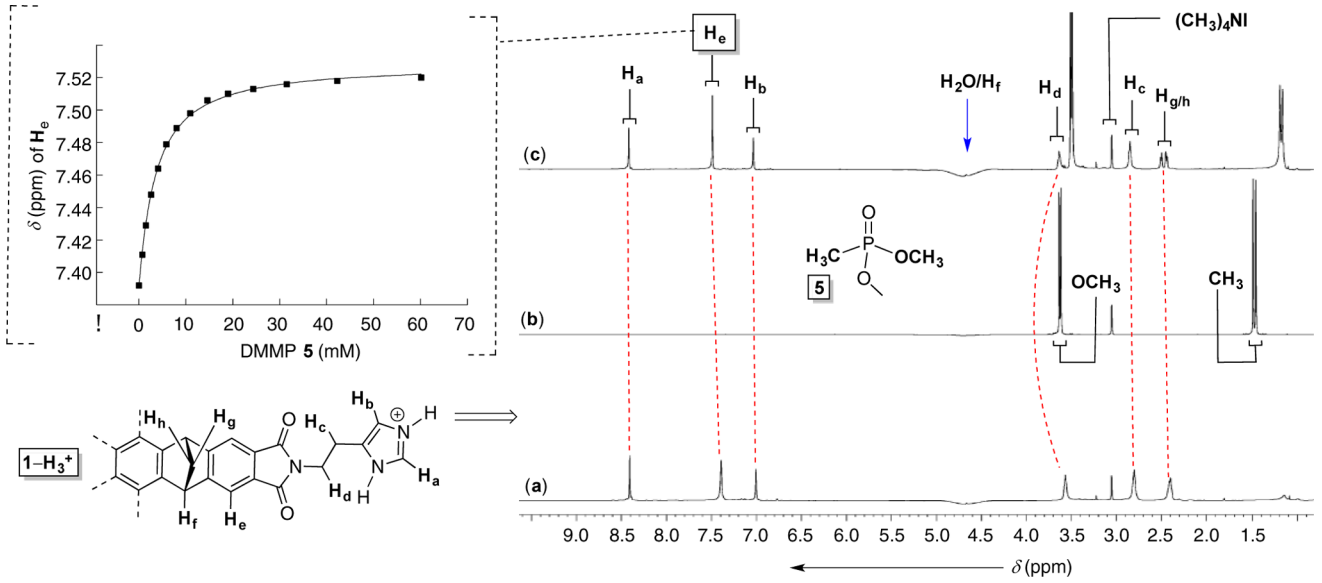

Figure 5. ^{1}H NMR spectra (600 MHz, water suppression) of (a) basket $[\mathbf{1}{-}\mathbf{H}_3]^{3+}$ (1.0 mM), (b) DMMP **5** and (c) their mixture (8.0 mM of **5**) in 10.0 mM phosphate buffer at pH = 2.5 ± 0.1. Nonlinear least-squares analysis of the binding data (298.0 K, 1:1 binding stoichiometry) gave the apparent association constant K_{app} = 321 ± 6 M^{-1} (R^2 = 0.999, SigmaPlot).

4): (a) the rotation about the central $CH_2{-}CH_2$ σ bond places the imidazole below (DOWN, Figure 4) or above (UP, Figure 4) the phthalimide, while (b) the rotation about the $N{-}CH_2$ linkage positions this same ring on the outer (OUT, Figure 4) or inner (IN, Figure 4) side of the basket's cavity. MD simulations (10 ns each) of $[\mathbf{1}{-}\mathbf{H}_3]^{3+}$ inside an octahedral box of TIP3P[73] water molecules placed within 10 Å of the basket gave numerous conformers that were all clustered into 10 principal groups (Figure 4B) by root-mean-square deviation (RMSD) procedures. The occurrence of different conformers is summarized with a contour plot comprising χ_1 and χ_2 torsions along the horizontal and vertical axis, respectively (Figure 4C); in the third dimension, the white designates absence while the red excess of the corresponding conformational states. In brief, the computational study suggests a greater abundance of baskets $[\mathbf{1}{-}\mathbf{H}_3]^{3+}$ with three imidazole moieties assuming UP/OUT, UP/IN and DOWN/OUT forms (Figure 4). The ^{1}H NMR spectrum of $[\mathbf{1}{-}\mathbf{H}_3]^{3+}$ showed a set of signals (600 MHz, 298.0 K) corresponding to a C_3 symmetric molecule (Figure 5); note that the assignment of proton resonances was assisted with NOE correlations (2D NOESY, Figure S3). Presumably, a rapid interconversion of different conformers of $[\mathbf{1}{-}\mathbf{H}_3]^{3+}$ on the NMR time scale[74] contributed to the signal averaging. The $CH_2{-}CH_2$ fragments in $[\mathbf{1}{-}\mathbf{H}_3]^{3+}$, however, appeared as two triplets with an averaged coupling constant of J = 6.3 Hz ($\mathbf{H}_c$/$\mathbf{H}_d$ protons, Figure 5). As in the case of $[\mathbf{4}{-}\mathbf{H}^+]$, this result supports the existence of anti/gauche conformers and is in agreement with our MD computational study (Figure 4). At pH = 2.5 ± 0.1, all three imidazoles ($pK_a \sim 6.9$) are protonated with (presumably) the positive charge keeping the residues apart; increasing the pH of water solution (pH ≥ 5) resulted in the precipitation of the basket.

The chemical shift of signals corresponding to imidazole protons $\mathbf{H}_{a/b}$ in $[\mathbf{1}{-}\mathbf{H}_3]^{3+}$ (δ = 7.0 and 8.4 ppm, Figure 5) are

dx.doi.org/10.1021/jp401841w | J. Phys. Chem. B 2013, 117, 3240−3249

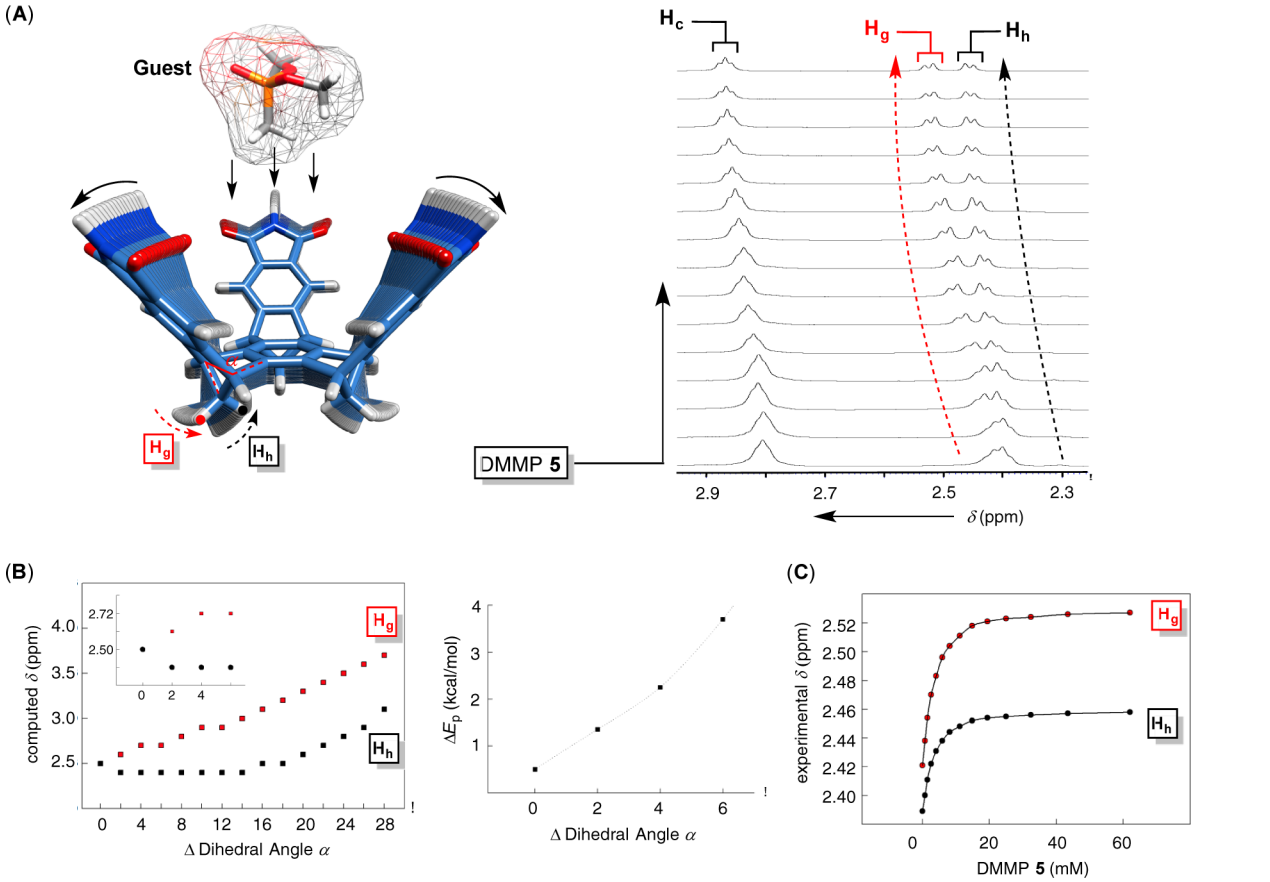

Figure 6. (A) A segment of the ^{1}H NMR spectra (600 MHz) of basket $[\mathbf{1}{-}\mathbf{H}_3]^{3+}$ (1.0 mM), obtained upon an incremental addition of DMMP **5** to its solution (10 mM phosphate buffer, pH = 2.5 ± 0.1). (B) Computed ^{1}H NMR chemical shifts of the bridge $\mathbf{H}_g/\mathbf{H}_h$ protons as a function of the dihedral angle α (top) as well as a variation in relative energies (ΔE, right) of these cup-shaped frameworks. (C) A plot showing a change in the chemical shift of bridge $\mathbf{H}_h/\mathbf{H}_g$ protons as a function of the concentration of DMMP **5**.

comparable to the corresponding resonances in the model compound $[\mathbf{4}{-}\mathbf{H}^+]$ (δ = 7.1 and 8.4 ppm, Figure S2). The absence of a strong magnetic shielding of these resonances in $[\mathbf{1}{-}\mathbf{H}_3{}^+]$ suggests that the imidazole moieties reside outside the basket's cavity. Furthermore, further dilution of a 1.0 mM aqueous solution of $[\mathbf{1}{-}\mathbf{H}_3{}^+]$ caused a small, but consistent, shift of all proton resonances (Figure S4). We reason that basket $[\mathbf{1}{-}\mathbf{H}_3{}^+]$, having a hydrocarbon framework, undergoes a self-aggregation in water to form labile assemblies in the examined range of concentrations (0.1−1.0 mM, Figure S4).

The Entrapment of DMMP 5. The incremental addition of dimethyl methylphosphonate **5** (DMMP) to basket $[\mathbf{1}{-}\mathbf{H}_3{}^+]$ (1.0 mM) dissolved in phosphate buffer (pH = 2.5 ± 0.1) caused a perturbation of the basket's ^{1}H NMR signals (Figure 5a−c). Specifically, all of the basket's resonances shifted downfield with the signal of $\mathbf{H}_e$ experiencing the greatest change ($\Delta\delta \sim 0.13$ ppm, Figure 5). The titration data were subjected to nonlinear least-squares analysis using a model describing the formation of a 1:1 host−guest complex at a fast rate.[75] The computed binding isotherm (at 298.0 K) fit well to the experimental data with the association constant of K_{app} = 321 ± 6 M^{-1} (Figure 5);[76] the 1:1 binding stoichiometry was also corroborated with the method of continuous variation (Figure S5).[77,78] Importantly, the addition of DMMP guest (60.0 mM) to an aqueous solution of model compound $[\mathbf{4}{-}\mathbf{H}^+]$ (14.3 mM) did not cause any change in its ^{1}H NMR spectrum (Figure S6).

Since there was no measurable interaction between the arm, $[\mathbf{4}{-}\mathbf{H}^+]$ (Figure 3), and DMMP, we conclude that the cavity in $[\mathbf{1}{-}\mathbf{H}_3]^{3+}$ must be critical for the observed recognition. What is the nature of the interaction between $[\mathbf{1}{-}\mathbf{H}_3]^{3+}$ and DMMP? First, one notes that the ^{1}H NMR signal corresponding to the bridge protons $\mathbf{H}_{g/h}$ from the host would decoalesce from a broad signal into an AB quartet with increasing amounts of DMMP guest (Figure 6A). The formation of the host−guest complex is, evidently, accompanied by structural/electronic changes to affect the magnetic environment of the bridge $\mathbf{H}_{g/h}$ protons. In particular, we surmised that docking of **5** inside $[\mathbf{1}{-}\mathbf{H}_3]^{3+}$ might require a small expansion/contraction of the basket's framework; indeed, flexing of the cup-shaped cage was previously computed[56] to create a small van der Waals strain (see Figure 6B), and this structural change is suggested to be potentially useful for an induced fit mechanism of the recognition.[79,80] In a series of DFT calculations (mPW1PW91/6-311+G**//mPW1PW91/6-31G*), we explored an alteration of the basket's dihedral angle α (Figure 6A) changing from 124° to 95° in 2° increments. This created a series of increasingly "open" cages, for which we computed ^{1}H NMR chemical shifts of $\mathbf{H}_{g/h}$ protons (Figure 6C).[81] The calculations suggested a greater deshielding of one proton nucleus (Figure 6B) with the expansion of the basket's framework. The result is consistent with our experimental measurements, whereby the resonances of two bridge protons underwent a disproportionate change with the addition of guest **5** (Figure 6C). Despite steric contacts, the complexation of

dx.doi.org/10.1021/jp401841w | J. Phys. Chem. B 2013, 117, 3240−3249

DMMP could also cause an electronic perturbation of the basket's framework to bring about the splitting of the bridge $H_{g/h}$ resonances. The magnitude of the electronic/steric effects in promoting the spectroscopic change is, at present, difficult to estimate, although our computational study is unequivocal about the basket's flexing contributing to the downfield ^{1}H NMR spectroscopic shift of the bridge protons.

As noted earlier, tetrahedral DMMP **5** could position one of its four groups in the cavity of $[\mathbf{1}{-}\mathbf{H}_3]^{3+}$ with the three remaining units pointing to the side apertures. Upon the complexation of this guest, the magnetic environment of P$-$C$\mathbf{H}_3$ ($\Delta\delta \sim 0.55$ ppm, Figure 7A) was apparently perturbed to

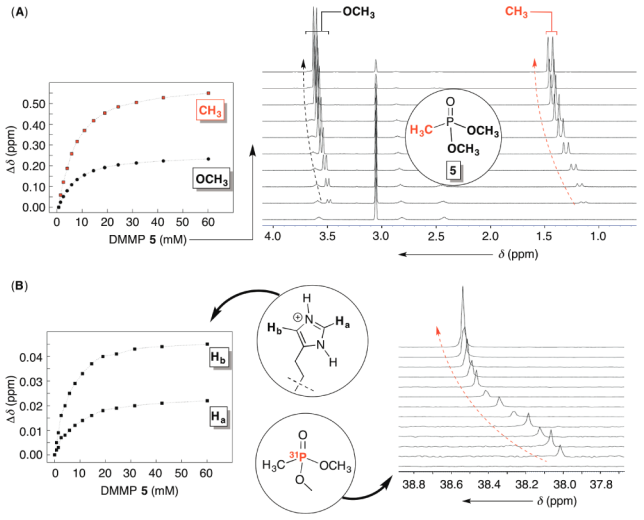

Figure 7. (A) ^{1}H NMR chemical shift of resonances corresponding to P$-$C$\mathbf{H}_3$ and P$-$OC$\mathbf{H}_3$ protons as a function of DMMP **5** titrated to $[\mathbf{1}{-}\mathbf{H}_3]^{3+}$ (1.0 mM). (B) ^{1}H NMR chemical shift of $\mathbf{H}_a/\mathbf{H}_b$ protons in $[\mathbf{1}{-}\mathbf{H}_3]^{3+}$ (left) and ^{31}P NMR shifts in DMMP **5** (right) as a function of the concentration of **5** titrated to $[\mathbf{1}{-}\mathbf{H}_3]^{3+}$ (1.0 mM).

a greater extent than that of P$-$OC$\mathbf{H}_3$ ($\Delta\delta \sim 0.22$ ppm, Figure 7A). A more considerable shielding of the C$\mathbf{H}_3$ protons suggests the positioning of this group in the cavity of $[\mathbf{1}{-}\mathbf{H}_3]^{3+}$ against the surrounding aromatic rings. In accord with this binding scenario, two methoxy groups reside between the carbonyl groups to, perhaps, experience their magnetic anisotropy. Furthermore, a small upfield shift of the phosphorus atom from DMMP **5** ($\Delta\delta \sim 0.6$ ppm, ^{31}P NMR; Figure 7B) is in line with P being magnetically shielded by the host. Finally, a small but measurable perturbation of the imidazole resonances $\mathbf{H}_a/\mathbf{H}_b$ ($\Delta\delta = 0.02{-}0.05$ ppm, Figure 7B) is an indication that these aromatic rings are barely interacting with the guest. Perhaps, a solvation shell of water molecules around the polar imidazolium groups is efficient in preventing their interaction with organophosphonate **5**. The formation of the $[\mathbf{1}{-}\mathbf{H}_3]^{3+} \subset$ **5** complex is followed by favorable enthalpy ($\Delta H^\circ = -1.60 \pm 0.08$ kcal/mol, 298.0 K) and entropy ($\Delta S^\circ = 6.3 \pm 0.9$ e.u., 298.0 K) as determined by calorimetric measurements (ITC, Figure S16). The enthalpy-driven interaction ($\Delta H^\circ < 0$) could be in line with an already proposed notion[82] that a hydration of apolar/concave surfaces is an unfavorable process contributing to the inclusion complexation (encapsulation) of organics in water.

To get more insight into the entrapment of DMMP **5** with $[\mathbf{1}{-}\mathbf{H}_3]^{3+}$, we docked this guest into 10 unique conformational states of the host (from MD simulations, see Supporting Information for additional details). Importantly, this protocol allowed us to assess a variety of docking poses and their favorability. Upon identifying 12 preferred modes of binding from molecular docking efforts, we resolvated each structure into an octahedral box of TIP3P water and then subjected each structure to an additional MD simulation (8 ns). Surprisingly, 11 out of 12 simulations gave rise to a complex whereby DMMP **5** places its P$-$C$\mathbf{H}_3$ group inside the cavity of $[\mathbf{1}{-}\mathbf{H}_3]^{3+}$ and toward the aromatic base of the host (Figure 8A, see

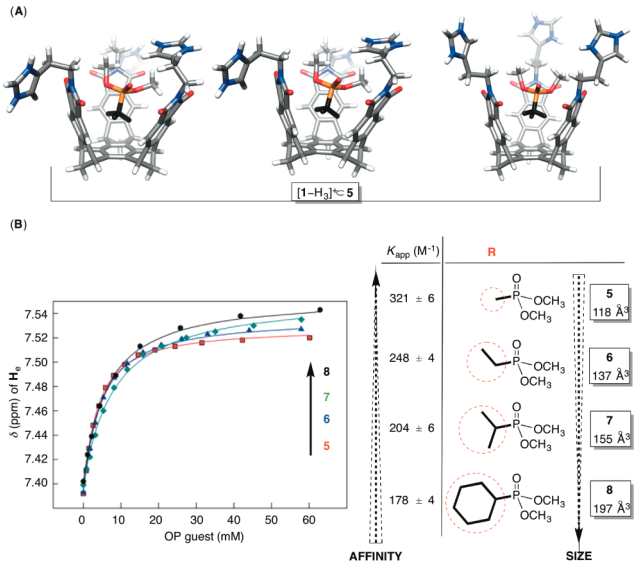

Figure 8. (A) Three different structures of $[\mathbf{1}{-}\mathbf{H}_3]^{3+} \subset$ **5** complex computed with molecular dynamics. (B) The interaction of **5**$-$**8** and $[\mathbf{1}{-}\mathbf{H}_3]^{3+}$ was examined with ^{1}H NMR spectroscopy (600 MHz) to give a series of apparent binding constants K_{app} (M^{-1}, 298.0 K) in 10.0 mM phosphate buffer (pH = 2.5 ± 0.1).

also a movie clip in Supporting Information). The computed orientation of the guest is in line with our NMR spectroscopic results, validating the importance of P$-$C$\mathbf{H}_3$ functionality for the recognition.

To further probe the entrapment of P$-\mathbf{R}$ alkyl groups from organophosphonates, we examined the affinity of guests **5**$-$**8** toward $[\mathbf{1}{-}\mathbf{H}_3^+]$ (Figure 8B). In particular, these guests carry increasingly larger R groups at the phosphorus center (Figure 8B). For this series of guests, the apparent binding affinity (K_{app}, Figure 6B) drops as the size of the R group increases! Evidently, the shallow cavity of basket $[\mathbf{1}{-}\mathbf{H}_3^+]$ accommodates C$\mathbf{H}_3$ more effectively than bulkier alkyl groups; the available data may also imply that methoxy groups in **7**/**8** start populating the host's cavity to a greater extent. The self-aggregation of $[\mathbf{1}{-}\mathbf{H}_3^+]$ (Figure S4) complicates the binding analysis, and these additional equilibria must be taken into account for obtaining binding constants (K_a). To simplify the matter, we kept the concentration of host $[\mathbf{1}{-}\mathbf{H}_3]^{3+}$ at 1.0 mM in all ^{1}H NMR titration experiments (Figure 8). To a first approximation, the measured apparent binding constants (K_{app}, Figure 8B) can now be compared, as the initial state is the same in all cases.

The Entrapment of Organophosphonates 9–13. The presence of the P$-$C$\mathbf{H}_3$ functionality within an organophosphonate guest is evidently important for the recognition. The remaining P$-$OR groups, however, would also need to be complementary to the host for forming a stable complex. To

dx.doi.org/10.1021/jp401841w | J. Phys. Chem. B 2013, 117, 3240−3249

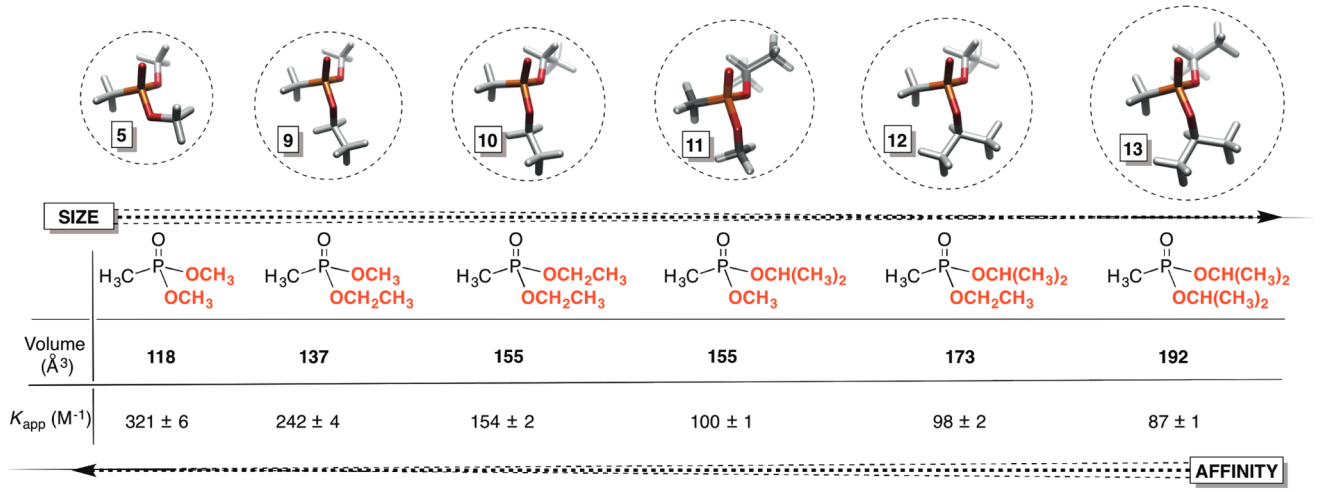

Figure 9. Energy-minimized structures of organophosphonates **5**/**9**−**13** (MMFFs, Spartan). The apparent binding affinities (K_{app}, M^{-1}) of **5**/**9**−**13** toward $[\mathbf{1}{-}\mathbf{H}_3]^{3+}$ (1.0 mM; 10.0 mM phosphate buffer at pH = 2.5 ± 0.1) were determined with ^{1}H NMR spectroscopy at 298.0 K.

assess the effect of the alkoxy substituents on the entrapment, we measured the affinity of guests **9**−**13** toward $[\mathbf{1}{-}\mathbf{H}_3^+]$ (Figure 9). Importantly, each guest in the series comprised an increasingly larger P−OR group (Figure 9). The apparent affinity descends in the series with DMMP **5** having the greatest (K_{app} = 321 ± 6 M^{-1}, Figure 9) while DIMP **13** (K_{app} = 87 ± 1 M^{-1}, Figure 9) has the lowest propensity for complexation with $[\mathbf{1}{-}\mathbf{H}_3^+]$. In essence, larger and more flexible alkoxy groups seem to impede the host−guest interactions to contribute to the binding trend; as we demonstrated in an earlier study,[83] this particular observation could have both enthalpic ($\Delta H°$, van der Waals strain) and entropic ($\Delta S°$, limited internal rotations) origins. When the ^{1}H NMR chemical shift of the P−CH_3 group in **5**/**9**−**13** was plotted against the amount of each guest titrated to the solution of $[\mathbf{1}{-}\mathbf{H}_3^+]$ (Figure 10A), an intriguing trend was observed: the stronger the host−guest interaction (K_{app}, Figure 10A), the more perturbed the magnetic environment of the methyl group in the guest (Figure 10A).

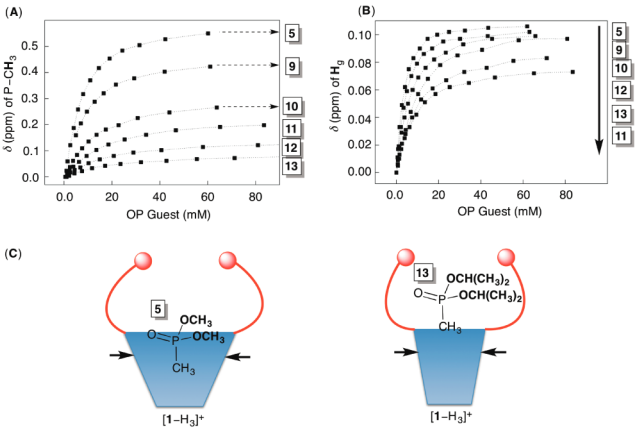

Figure 10. (A) ^{1}H NMR chemical shift of P−CH_3 in **5**/**9**−**13** as a function of the concentration of guest compounds titrated to 1.0 mM solution of $[\mathbf{1}{-}\mathbf{H}_3]^{3+}$ (10 mM phosphate buffer, pH = 2.5 ± 0.1). (B) ^{1}H NMR chemical shift of bridge $\mathbf{H}_g$ proton (see Figure 6) in $[\mathbf{1}{-}\mathbf{H}_3]^{3+}$ as a function of **5**/**9**−**13** added to its 1.0 mM solution. (C) It appears that smaller organophosphonate **5** has a greater access to the basket's inner space than bigger **13** causing a disproportionate expansion of the cup-shaped framework.

To explain this observation, we further considered relative ^{1}H NMR chemical shifts of the bridge $\mathbf{H}_g$ proton (Figure 6) in $[\mathbf{1}{-}\mathbf{H}_3^+]$ entrapping **5**/**9**−**13** (Figure 10B). As noted earlier, ^{1}H NMR chemical shifts of the host's bridge nuclei signify a degree of the basket's expansion/contraction. In the **5**/**9**−**13** series, larger alkoxy guests caused a smaller change in the chemical shift of the host's bridge $\mathbf{H}_g$ proton (Figure 10B). We surmise that the host undergoes a different conformational adjustment to each particular organophosphonates as a guest. Specifically, guest **5** with smaller methoxy units (Figure 10C) accesses the southern portion of $[\mathbf{1}{-}\mathbf{H}_3]^{3+}$ more effectively by placing its P−CH_3 group in the cavity, and directly at the aromatic base of the host. This, in turn, causes the cup-shaped platform to expand its arms. On the contrary, organophosphonate **13** with larger alkoxy units (Figure 10C) could not effectively reach the inner space of $[\mathbf{1}{-}\mathbf{H}_3]^{3+}$, causing a smaller expansion of the cup-shaped platform (Figure 10C) and thereby a smaller disturbance of the magnetic environment of the P−CH_3 moiety.

CONCLUSION

Modular basket-like hosts entrap a variety of organophosphonate compounds with shape and size corresponding to chemical warfare agents. The binding takes place in water with structure−activity relationships that stress the importance of steric interactions for fine-tuning the chemoselectivity. Interestingly, experimental methods suggest an induced-fit mechanism of the recognition whereby the basket's framework is flexing to a variable degree for accommodating the P−CH_3 group from the guest compound. The stage is now set for improving the selectivity and affinity of baskets toward CWA's.

ASSOCIATED CONTENT

Supporting Information

Additional details of the experimental and computational protocols. This material is available free of charge via the Internet at http://pubs.acs.org.

AUTHOR INFORMATION

Corresponding Author

*E-mail: badjic@chemistry.ohio-state.edu; E-mail: hadad.1@osu.edu. Fax: 614 292 1685; Tel: 614 247 8342

Notes

The authors declare no competing financial interest.

■ ACKNOWLEDGMENTS

We thank Professor Hans J. Reich (University of Wisconsin) for useful suggestions. This work was financially supported with funds obtained from the National Science Foundation (CHE-1012146, to J.D.B.) and the Department of Defense, Defense Threat Reduction Agency (HDTRA1-11-1-0042, to J.D.B. and C.M.H.). The content of the information does not necessarily reflect the position or the policy of the federal government, and no official endorsement should be inferred. The Ohio Supercomputer Center is gratefully acknowledged for providing generous computational resources.

■ REFERENCES

(1) Holstege, C. P.; Kirk, M.; Sidell, F. R. *Crit. Care Clin.* **1997**, *13*, 923.
(2) Burdon, J. *Mol. Death* **2002**, 139.
(3) Sadik, O. A.; Land, W. H., Jr.; Wang, J. *Electroanalysis* **2003**, *15*, 1149.
(4) Chauhan, S.; Chauhan, S.; D'Cruz, R.; Faruqi, S.; Singh, K. K.; Varma, S.; Singh, M.; Karthik, V. *Environ. Toxicol. Pharmacol.* **2008**, *26*, 113.
(5) Sawyer, T. W.; Weiss, M. T.; Boulet, C. A.; Hansen, A. S. *Fundam. Appl. Toxicol.* **1991**, *17*, 208.
(6) Bajgar, J. *Adv. Clin. Chem.* **2004**, *38*, 151.
(7) Bajgar, J.; Kuca, K.; Jun, D.; Bartosova, L.; Fusek, J. *Curr. Drug Metab.* **2007**, *8*, 803.
(8) Pope, C.; Karanth, S.; Liu, J. *Environ. Toxicol. Pharmacol.* **2005**, *19*, 433.
(9) Montoro, C.; Linares, F.; Quartapelle Procopio, E.; Senkovska, I.; Kaskel, S.; Galli, S.; Masciocchi, N.; Barea, E.; Navarro, J. A. R. *J. Am. Chem. Soc.* **2011**, *133*, 11888.
(10) Lejeune, K. E.; Dravis, B. C.; Yang, F.; Hetro, A. D.; Doctor, B. P.; Russell, A. J. *Ann. N.Y. Acad. Sci.* **1998**, *864*, 153.
(11) Burnworth, M.; Rowan, S. J.; Weder, C. *Chem.—Eur. J.* **2007**, *13*, 7828.
(12) Kim, K.; Tsay, O. G.; Atwood, D. A.; Churchill, D. G. *Chem. Rev.* **2011**, *111*, 5345.
(13) Yang, Y. C.; Baker, J. A.; Ward, J. R. *Chem. Rev.* **1992**, *92*, 1729.
(14) Talmage, S. S.; Watson, A. P.; Hauschild, V.; Munro, N. B.; King, J. *Curr. Org. Chem.* **2007**, *11*, 285.
(15) Prasad, G. K. *Nanotechnol. Environ. Decontam.* **2011**, 193.
(16) Smith, B. M. *Chem. Soc. Rev.* **2008**, *37*, 470.
(17) Liu, C. T.; Neverov, A. A.; Maxwell, C. I.; Brown, R. S. *J. Am. Chem. Soc.* **2010**, *132*, 3561.
(18) Um, I.-H.; Shin, Y.-H.; Lee, S.-E.; Yang, K.; Buncel, E. *J. Org. Chem.* **2008**, *73*, 923.
(19) Cordell, R. L.; Willis, K. A.; Wyche, K. P.; Blake, R. S.; Ellis, A. M.; Monks, P. S. *Anal. Chem.* **2007**, *79*, 8359.
(20) Creasy, W.; Fry, R.; McGarvey, D.; Hendrickson, D.; Durst, H. D. *Main Group Chem.* **2010**, *9*, 245.
(21) Aleksenko, S. S.; Gareil, P.; Timerbaev, A. R. *Analyst* **2011**, *136*, 4103.
(22) Gunzer, F.; Zimmermann, S.; Baether, W. *Anal. Chem.* **2010**, *82*, 3756.
(23) Wallace, K. J.; Morey, J.; Lynch, V. M.; Anslyn, E. V. *New J. Chem.* **2005**, *29*, 1469.
(24) Royo, S.; Martinez-Manez, R.; Sancenon, F.; Costero, A. M.; Parra, M.; Gil, S. *Chem. Commun.* **2007**, 4839.
(25) Costero, A. M.; Gil, S.; Parra, M.; Mancini, P. M. E.; Martinez-Manez, R.; Sancenon, F.; Royo, S. *Chem. Commun.* **2008**, 6002.
(26) Gotor, R.; Costero, A. M.; Gil, S.; Parra, M.; Martinez-Manez, R.; Sancenon, F. *Chem.—Eur. J.* **2011**, *17*, 11994.
(27) Lee, J.; Seo, S.; Kim, J. *Adv. Funct. Mater.* **2012**, *22*, 1632.
(28) Wu, Z.; Wu, X.; Yang, Y.; Wen, T.-b.; Han, S. *Bioorg. Med. Chem. Lett.* **2012**, *22*, 6358.
(29) Wallace, K. J.; Fagbemi, R. I.; Folmer-Andersen, F. J.; Morey, J.; Lynth, V. M.; Anslyn, E. V. *Chem. Commun.* **2006**, 3886.
(30) Wild, A.; Winter, A.; Hager, M. D.; Schubert, U. S. *Chem. Commun.* **2012**, *48*, 964.
(31) Walton, I.; Davis, M.; Munro, L.; Catalano, V. J.; Cragg, P. J.; Huggins, M. T.; Wallace, K. J. *Org. Lett.* **2012**, *14*, 2686.
(32) Morales-Rojas, H.; Moss, R. A. *Chem. Rev.* **2002**, *102*, 2497.
(33) Dale, T. J.; Rebek, J., Jr. *J. Am. Chem. Soc.* **2006**, *128*, 4500.
(34) Dale, T. J.; Rebek, J., Jr. *Angew. Chem., Int. Ed.* **2009**, *48*, 7850.
(35) Zhang, S.-W.; Swager, T. M. *J. Am. Chem. Soc.* **2003**, *125*, 3420.
(36) Chulvi, K.; Gavina, P.; Costero, A. M.; Gil, S.; Parra, M.; Gotor, R.; Royo, S.; Martinez-Manez, R.; Sancenon, F.; Vivancos, J.-L. *Chem. Commun.* **2012**, *48*, 10105.
(37) Kitamura, M.; Shabbir, S. H.; Anslyn, E. V. *J. Org. Chem.* **2009**, *74*, 4479.
(38) Lim, S. H.; Feng, L.; Kemling, J. W.; Musto, C. J.; Suslick, K. S. *Nat. Chem.* **2009**, *1*, 562.
(39) Hargrove, A. E.; Nieto, S.; Zhang, T.; Sessler, J. L.; Anslyn, E. V. *Chem. Rev.* **2011**, *111*, 6603.
(40) Sambrook, M. R.; Hiscock, J. R.; Cook, A.; Green, A. C.; Holden, I.; Vincent, J. C.; Gale, P. A. *Chem. Commun.* **2012**, *48*, 5605.
(41) Badjic, J. D.; Stojanovic, S.; Ruan, Y. *Adv. Phys. Org. Chem.* **2011**, *45*, 1.
(42) Cram, D. J. *Science* **1983**, *219*, 1177.
(43) Cram, D. J. *Science* **1988**, *240*, 760.
(44) Hennrich, N.; Cramer, F. *J. Am. Chem. Soc.* **1965**, *87*, 1121.
(45) Van Hooidonk, C.; Groos, C. C. *Recl. Trav. Chim. Pays-Bas* **1970**, *89*, 845.
(46) Van Hooidonk, C.; Breebaart-Hansen, J. C. A. E. *Recl. Trav. Chim. Pays-Bas* **1970**, *89*, 289.
(47) Desire, B.; Saint-Andre, S. *Fundam. Appl. Toxicol.* **1986**, *7*, 646.
(48) Desire, B.; Saint-Andre, S. *Experientia* **1987**, *43*, 395.
(49) Le Provost, R.; Wille, T.; Louise, L.; Masurier, N.; Mueller, S.; Reiter, G.; Renard, P.-Y.; Lafont, O.; Worek, F.; Estour, F. *Org. Biomol. Chem.* **2011**, *9*, 3026.
(50) Wille, T.; Tenberken, O.; Reiter, G.; Muller, S.; Le Provost, R.; Lafont, O.; Estour, F.; Thiermann, H.; Worek, F. *Toxicology* **2009**, *265*, 96.
(51) Zengerle, M.; Brandhuber, F.; Schneider, C.; Worek, F.; Reiter, G.; Kubik, S. *Beilstein J. Org. Chem.* **2011**, *7*, 1543.
(52) Daly, S. M.; Grassi, M.; Shenoy, D. K.; Ugozzoli, F.; Dalcanale, E. *J. Mater. Chem.* **2007**, *17*, 1809.
(53) Tudisco, C.; Betti, P.; Motta, A.; Pinalli, R.; Bombaci, L.; Dalcanale, E.; Condorelli, G. G. *Langmuir* **2012**, *28*, 1782.
(54) Rieth, S.; Hermann, K.; Wang, B.-Y.; Badjic, J. D. *Chem. Soc. Rev.* **2011**, *40*, 1609.
(55) Maslak, V.; Yan, Z.; Xia, S.; Gallucci, J.; Hadad, C. M.; Badjic, J. D. *J. Am. Chem. Soc.* **2006**, *128*, 5887.
(56) Yan, Z.; McCracken, T.; Xia, S.; Maslak, V.; Gallucci, J.; Hadad, C. M.; Badjic, J. D. *J. Org. Chem.* **2008**, *73*, 355.
(57) Rieth, S.; Yan, Z.; Xia, S.; Gardlik, M.; Chow, A.; Fraenkel, G.; Hadad, C. M.; Badjic, J. D. *J. Org. Chem.* **2008**, *73*, 5100.
(58) Yan, Z.; Xia, S.; Gardlik, M.; Seo, W.; Maslak, V.; Gallucci, J.; Hadad, C. M.; Badjic, J. D. *Org. Lett.* **2007**, *9*, 2301.
(59) Wang, B.-Y.; Rieth, S.; Badjic, J. D. *J. Am. Chem. Soc.* **2009**, *131*, 7250.
(60) Wittenberg, J. B.; Isaacs, L. *Supramol. Chem. Mol. Nanomater.* **2012**, *1*, 25.
(61) Gan, H.; Gibb, B. C. *Chem. Commun.* **2012**, *48*, 1656.
(62) Gibb, B. C. *Chemosensors* **2011**, 3.
(63) Godec, A.; Merzel, F. *J. Am. Chem. Soc.* **2012**, *134*, 17574.
(64) Ponnuswamy, N.; Cougnon, F. B. L.; Clough, J. M.; Pantos, G. D.; Sanders, J. K. M. *Science* **2012**, *338*, 783.
(65) Gerst, K.; Nordman, C. E. *Acta Crystallogr., Sect. B* **1977**, *B33*, 1588.
(66) Acharya, J.; Shakya, P. D.; Pardasani, D.; Palit, M.; Dubey, D. K.; Gupta, A. K. *J. Chem. Res.* **2005**, 194.

(67) Reichwein, J. F.; Pagenkopf, B. L. *J. Org. Chem.* **2003**, *68*, 1459.
(68) Sutter, P.; Weis, C. D. *J. Heterocycl. Chem.* **1980**, *17*, 493.
(69) Guenther, H. *Angew. Chem., Int. Ed. Engl.* **1972**, *11*, 861.
(70) Whitesides, G. M.; Sevenair, J. P.; Goetz, R. W. *J. Am. Chem. Soc.* **1967**, *89*, 1135.
(71) Gregoire, F.; Wei, S. H.; Streed, E. W.; Brameld, K. A.; Fort, D.; Hanely, L. J.; Walls, J. D.; Goddard, W. A.; Roberts, J. D. *J. Am. Chem. Soc.* **1998**, *120*, 7537.
(72) Reich, H. J. Private communication, see: http://www.chem.wisc.edu/areas/reich/chem605/index.htm, 2012.
(73) Jorgensen, W. L.; Chandrasekhar, J.; Madura, J. D.; Impey, R. W.; Klein, M. L. *J. Chem. Phys.* **1983**, *79*, 926.
(74) Hermann, K.; Rieth, S.; Taha, H. A.; Wang, B.-Y.; Hadad, C. M.; Badjic, J. D. *Beilstein J. Org. Chem.* **2012**, *8*, 90.
(75) Schneider, H. J.; Duerr, H., Ed. *Frontiers in Supramolecular Organic Chemistry and Photochemistry*: Wiley-VCH: Weinheim, Germany, 1991.
(76) Thordarson, P. *Chem. Soc. Rev.* **2011**, *40*, 1305.
(77) Hirose, K. *J. Inclusion Phenom. Macrocyclic Chem.* **2001**, *39*, 193.
(78) Hirose, K. *Anal. Methods Supramol. Chem.* **2007**, 17.
(79) Bucher, D.; Grant, B. J.; McCammon, J. A. *Biochemistry* **2011**, *50*, 10530.
(80) Vogt, A. D.; Di Cera, E. *Biochemistry* **2012**, *51*, 5894.
(81) Lodewyk, M. W.; Siebert, M. R.; Tantillo, D. J. *Chem. Rev.* **2012**, *112*, 1839.
(82) Meyer, E. A.; Castellano, R. K.; Diederich, F. *Angew. Chem., Int. Ed.* **2003**, *42*, 1210.
(83) Wang, B.-Y.; Bao, X.; Stojanovic, S.; Hadad, C. M.; Badjic, J. D. *Org. Lett.* **2008**, *10*, 5361.